



Surface roughness as the function of friction indicator and an important parameters-combination having controlling influence on the roughness: recent results in incremental forming

Hongyu Wei¹ · G. Hussain^{2,3} · A. Iqbal⁴ · Z. P. Zhang¹

Received: 11 July 2018 / Accepted: 20 November 2018 / Published online: 4 December 2018
© Springer-Verlag London Ltd., part of Springer Nature 2018

Abstract

Surface roughness affects the performance and service life of the formed components. To this end, efforts have been spent in the innovative incremental sheet forming (ISF) process. However, the researchers yet have not reached any agreement regarding the process effects on roughness. This demands further research to comprehend the knowledge in order to acquire a threshold level of understanding on surface roughening in the process. The present study investigates the processing effects upon the roughness of interior surfaces and on the friction indicator at the tool/sheet interface during forming of an aluminum sheet. Some of the sparsely studied parameters, namely flow stress, sheet thickness, and forming angle, are undertaken besides commonly considered ones (i.e., tool diameter and step size). The analysis of the results reveals that the friction indicator and roughness are analogous in respect of their response to parameter variations. Further, the roughness in general linearly increases with an increase in the friction indicator because the sheet abrasion correspondingly increases as revealed by the SEM-based surface morphology. A combination of parameters, among several attempted ones, namely $d\sin\theta/2pt$ (where d is the tool diameter, θ is the forming angle, p is the step size, and t is the sheet thickness), is identified to have controlling influence on the roughness of interior surfaces. This combination is validated employing two materials namely Al1060 and Cu/Steel composite. In this combination, the factor $d/2p$ followed by $1/t$ is found to have the greatest contribution towards the roughening of surfaces. Moreover, the value of this combination is proposed to keep low in order to produce components with good finish, say $\leq 50 \text{ mm}^{-1}$ for Al10160 and 20 mm^{-1} for Cu/Steel composite. The present and past roughness studies in ISF are also compared, which reveals that the parameters effects are associated to the type of material.

Keywords Incremental forming · Friction indicator · Surface roughness · Surface morphology · Parameter-combination

1 Introduction

Incremental sheet forming (ISF) is an innovative sheet forming process with high economic pay off for small production runs. The process performs forming without utilizing the shape-dependent dies. Because of offering this flexibility, ISF is gaining popularity in the biomedical and automotive sectors

[1, 2]. A great deal of efforts are being spent to realize the process deployment on the industrial scale [3–6]. The latest developments in the process have been comprehensively detailed in a number of review papers [7–9].

Surface quality is paid substantial attention in metal forming, because it does affect not only the esthetic look of a component but also the performance and service life. To this end, a number of

✉ G. Hussain
gh_ghumman@hotmail.com

Hongyu Wei
whyme@nuaa.edu.cn

A. Iqbal
asif.asifiqbal@gmail.com

Z. P. Zhang
15850722983@163.com

¹ College of Mechanical & Electrical Engineering, Nanjing University of Aeronautics & Astronautics, Nanjing, People's Republic of China

² Faculty of Mechanical Engineering, GIK Institute of Engineering Sciences & Technology, KP, Topi 23640, Pakistan

³ Visiting Scholar, College of Mechanical & Electrical Engineering, Nanjing University of Aeronautics & Astronautics, Nanjing, People's Republic of China

⁴ Faculty of Integrated Technologies, University of Brunei Darussalam Jalan Tungku Link, Bandar Seri Begawan BE1410, Brunei Darussalam

works have been performed to control the surface quality in ISF. Some researchers attempted to enhance the surface quality employing tools with the rolling end and appropriate lubricant [10–13], some relied on the tool path strategy [14], while the others opted for an optimum set of processing conditions. The last approach has been the most adopted one to enhance the surface quality of interior surfaces (i.e., surface in contact with the forming tool). A summary of these efforts is presented as follows.

While studying the influence of step size, Hagan and Jeswiet [15] found that the roughness increased as the step size increased from 0.05 to 1.5 mm. This finding was later endorsed by Echrif et al. [16] and Durante et al. [17] with step size ranging from 0.25 to 1 mm and from 0.2 to 0.6 mm, respectively. Mugendiran et al. [18] and Cavalier et al. [19] reported an opposite trend for the step size respectively ranging from 0.35 to 0.5 mm and 0.4 to 0.8 mm. Extending the investigation, Baruah et al. [20] observed an increase in the roughness for the range of 0.2 to 0.5 mm, while a decrease for the range of 0.5 to 0.9 mm. As those on the effect of step size on roughness, diverse observations have been reported regarding the effect of spindle rotation also. Hagan and Jeswiet [15] found that the roughness decreased as the rotational speed was increased from 0 to 1500 rpm and contrarily increased when the speed was further increased from 1500 to 2600 rpm. Durante et al. [21] observed a decrease in the roughness with increasing rotation up to 600 rpm. Echrif et al. [16] reported an increase in the roughness for the rotation ranging from 500 to 2000 rpm. Mugendiran et al. [18] recorded a reduction in the roughness at the rotation ranging from 1700 to 2000 rpm followed by an increase at greater rotations (i.e., from 2000 to 2300 rpm). A similar trend was witnessed by Baruah et al. [20] but comparatively at lower speeds (i.e., from 150 to 400 rpm and from 400 to 800 rpm).

Like that of rotation, the influence of feed rate on the roughness has also not been agreed upon. According to Echrif et al. [16], the roughness increases as the feed increases from 500 to 1500 mm/min. Baruah et al. [20] and Mugendiran et al. [18], however, claim an opposite effect for the feed respectively ranging from 200 to 800 mm/min and 500 to 650 mm/min. As regards the tool diameter, Echrif et al. [16] and Durante et al. [17] have proposed to employ greater diameters (say from 5 to 30 mm) to minimize roughness. Cavalier et al. [19], however, propose the opposite specifically when the diameter ranges from 8 to 10 mm.

The reported studies provide thoughtful insights into the roughening behavior of interior surface in ISF. However, there is a need to gather more information for having better control on the process. In this regards, the contribution of flow stress of material and forming angle on surface roughening is very particular to be revealed because these parameters are likely to affect the strain hardening and thus the sheet wear and surface roughness. Moreover, as clear from the gap analysis presented in Table 1, investigations regarding the sheet thickness effect are also scarce. Besides these points, due to discrepancies in

the published reports as highlighted before, the nature of effects of parameters on roughness is yet a subject of debate. Therefore, further studies by widening the type (and range) of parameters and materials are required to adequately comprehend the roughening behavior of materials in ISF.

Recently, a number of researchers have identified that the friction indicator is an important factor with significant effect on the roughness in ISF [17, 21, 22]. However, this factor has been mainly studied as the function of rotational speed. The friction indicator as the function of remainder processing parameters along with the associated effect on the roughness also requires thorough investigation in order to exhaustively understand the role of friction on roughening in ISF.

Hamilton and Jeswiet [23], while analyzing the roughness of exterior surface (free surface) of formed Al3003 sheet, proposed that an empirical combination of tool radius, forming angle, and step size has controlling influence on the equivalent roughness in ISF. However, its application to the interior surface (surface in contact with tool) and extension to other materials yet need to be ascertained. Further, a more appropriate and robust combination should be devised if the proposed one does not describe the roughening behavior of interior surfaces.

From the above discussion, it follows that there is a need to perform a systematic study in order to fill the indicated gaps. The five forming parameters (i.e., flow stress, forming angle, sheet thickness, tool diameter, and step size) are varied over wide ranges and their effects on the friction indicator and roughness of interior surface are quantified and analyzed. In an attempt to identify the most appropriate parameter-combination having controlling influence on the roughening of interior surface, a number of trials are attempted and a new robust combination is proposed. Moreover, the roughness findings of the current study are compared with those of the past studies and important inferences are drawn.

2 Methodology

The past works [9] have revealed that the performance of ISF process largely relies on the complex inter-dependent effects of technological conditions, and further, an ad hoc approach is unable to furnish adequate information to control the process. The statistical approaches, therefore, have been applied to realize the solution. To analyze the friction indicator and roughness, the response surface method (one of the statistical approaches) was adopted in this study. More in detail, the central composite design (CCD) was opted among various response surface designs as this evenly distributes the design points [24].

The following parameters were the predictors of CCD:

- Flow stress of material (Y_f in MPa)
- Sheet thickness (t in mm)
- Forming angle (θ in degrees)

Table 1 Gap analysis and comparison between the current and past studies. The values alongside the arrows represent the range of particular parameter under study

	Hagan and Jeswiet [15]	Mugendiran et al. [18]	Echrf et al. [16]	Durante et al. [17, 21]	Cavaler et al. [19]	Baruah et al. [20]	Current study		
Material	Al3003	Al5052	Al1050O	Al7075O	AISI304L	Al5052	Al1060		
Response	R_a (μm)	R_a (μm)	R_a (μm)	R_a (μm)	R_a (μm)	R_a (μm)	R_a (μm)	R_{eqv} (μm)	μ'
p- step size (mm)	↑ 0.05-1.5	↓ 0.35-0.5 ↑ 0.5-0.65	↑ 0.25-1	↑ 0.2-0.6	↓ 0.4-0.8	↑ 0.2-0.5 ↓ 0.5-0.9	↑ 0.1-0.8	↑ (0.1-0.8)	↑ 0.1-0.8
d- diameter (mm)	—	—	↓ 5-30	↓ 5-15	↑ 8-10	—	↓ 7-13.5 ↑ 13.5-20	↓ 7-20	↑ 7-13.5 ↑ 13.5-20
t - thickness (mm)	—	—	—	—	—	—	↑ 0.7-2.6	↑	↑ 0.7-2.6 (d ≤ 17mm) (θ ≤ 47°)
θ- angle (deg)	—	—	—	—	—	—	↓ 28-55 ↑ 20-28	↓	↓ t ≥ 1.2mm d ≤ 17mm
Y_f stress (MPa)	—	—	—	—	—	—	↓ 101-172	→	→
ω- rotation (rpm)	↓ 0-1500 ↑ 1500-2600	↓ 1700-2000 ↑ 2000-2300	↑ 500-2000	↓ 0-600	—	↓ 150-400 ↑ 400-800	—	—	—
f- feed (mm/min)	—	↓ 500-650 ↑ 650-800	↑ 500-1500	—	—	↓ 200-800	—	—	—
Range	0.5-4.5	1.92-5.28	0.37-17.5	0.4-9.2	0.9-1.44	0.33-1	0.095-3.97	0.004-4.37	0.196-1.25

Key: ↑ increase; ↓ decrease; → no effect; — not investigated

Tool diameter (d in mm)
Step size (p in mm)

The reader is referred to Fig. 1a for the illustration of these parameters. As indicated in the list of parameters, the flow stress of material and forming angle was also undertaken in line with the objective of current study. The tool rotation and feed rate are among the important parameters of ISF process. Their influence on the roughness may depend on the type of material [16, 18]. These parameters in the present study, however, were kept fixed to 0 rpm and 2600 mm/min, respectively. Because, a special-built non-rotational post was utilized to hold the forming tool, and further, there was a constraint on the available material. The range(s) of other parameters selected for the investigation have been presented in Table 1. These ranges were set according to the machine specifications and available resources. To prepare the test plan and for analyzing the roughness, a commercial statistics package Design Expert Dx-10 was utilized.

Table 2 shows the complete test plan. The plan is composed of 47 runs, whereby each of the parameters has three levels. The plan also contains five replicates to consider repeatability. This plan, consistent with the

objective of current study, was intended to investigate the following friction and roughness variables:

- Friction indicator (μ')
- Arithmetic mean roughness (R_a in μm)
- 10 points average roughness (R_z in μm)
- Maximum peak-valley roughness (R_{max} in μm)
- Equivalent roughness (R_{eqv} in μm)

Because of its extensive structural applications, the commercial aluminum sheet AA1060 was employed as the experimental material. The sheet material, which ranged from 0.7 to 2.6 mm in thickness, was received in the rolled condition. Therefore, it was annealed over two different temperatures (285 and 320 °C) in order to achieve two additional levels of flow stress. The annealing was done by holding the sheet for 2 h in the carbolite furnace. To determine the flow stress, the tensile specimens were prepared following the ASTM E8 standard [25] and stretched to fracture utilizing a universal testing machine and employing the crosshead speed of 2 mm/min. To obtain precise results, each test was repeated twice. In order to consider the anisotropy effects, the tests

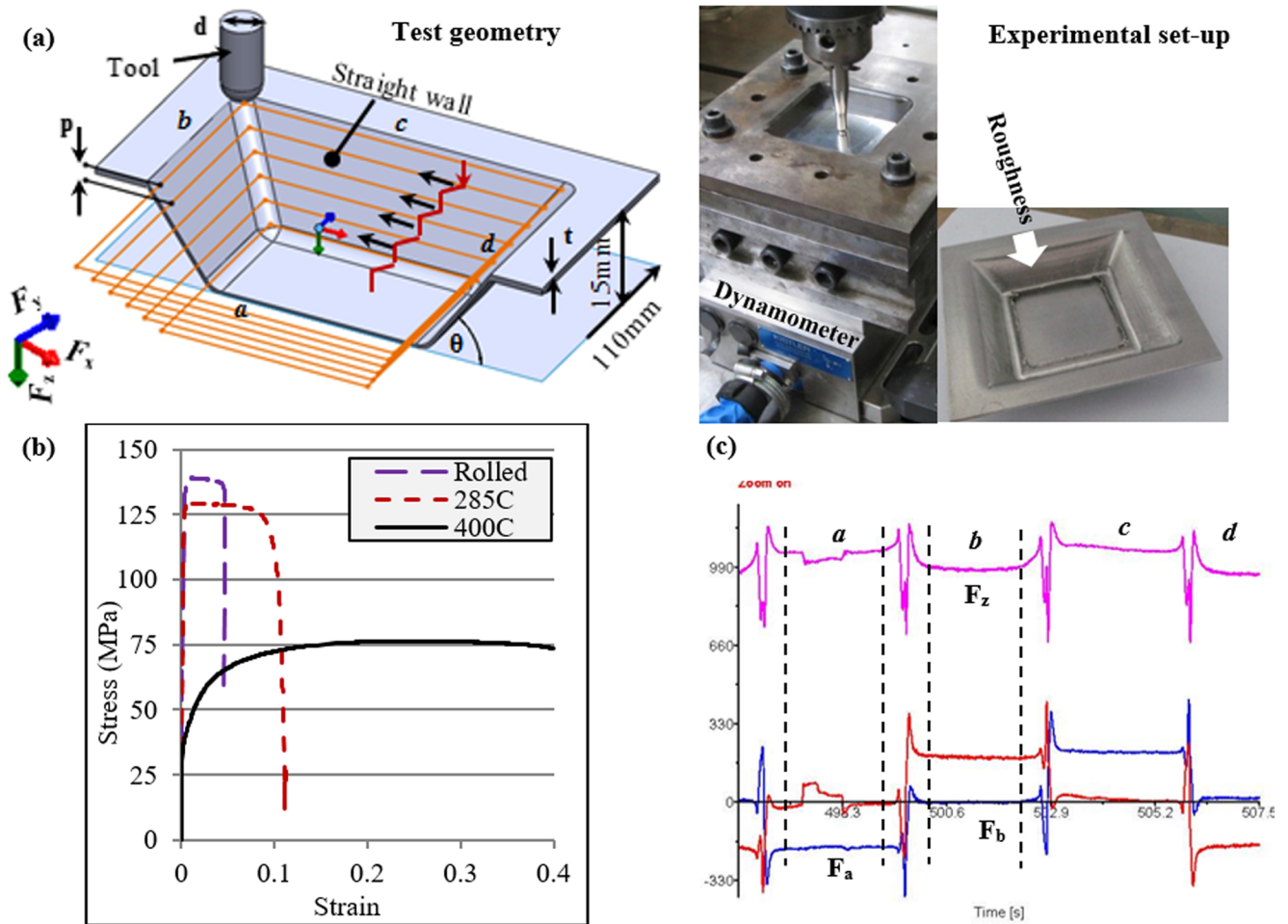


Fig. 1 Experimental and material details: **a** test geometry and experimental set-up, **b** engineering stress-strain curves of material, and **c** a representative case of force measurement

were carried out in both of the rolling and transverse directions. Figure 1b shows the representative stress/strain curves in the rolling direction. The mean flow stress (stress required to flow the material) of material against each of the material conditions was determined using the below formula:

$$Y_f = \frac{K\varepsilon^n}{n + 1} \tag{1}$$

where Y_f (MPa) is the mean flow stress over the entire strain history, K (MPa) is the strength coefficient, n is the strain rate exponent, and ε is the true strain at fracture. The values of n and K were determined by plotting the stress and strain data on logarithmic scale. The average value of Y_f was obtained by summing up the flow stress in the rolling and transverse directions. The maximum deviation in Y_f was recorded to be ± 3 MPa.

To study the friction and roughness, the sheet was formed into a simple pyramid shape as depicted in Fig. 1a. For this purpose, the sheet blank (140 mm \times 140 mm) was clamped onto a fixture and the forming tool was programmed to follow a pre-defined trajectory on a 3-axis CNC milling machine.

During forming, the mineral oil was used as a lubricant to reduce friction at the tool/sheet interface. In order to characterize friction at the tool/sheet interface, the forming forces were measured in the X , Y , and Z directions. For this purpose, a table type dynamometer (9625B) was installed under the forming rig (Fig. 1a), and the forces were recorded through the data acquisition system. The snapshot of representative force curves is shown in Fig. 1c.

It is a difficult task to find the exact value of friction coefficient during ISF. Therefore, an indicator of friction was calculated to represent friction, as defined in Durante et al. [21] and given below:

$$\mu' = \frac{|F_h|}{|F_z|} \tag{2}$$

where μ' is the friction indicator.

- F_h (N) is the horizontal (or in-plane) force that resists the motion of forming tool in the horizontal plane.
- F_z (N) is the vertical force that acts normal to the horizontal plane (x - y) and flattens the sheet.

Table 2 The test plan composed of 47 tests

<i>t</i> (mm)	<i>θ</i> (deg)	<i>Y_f</i> (MPa)	<i>d</i> (mm)	<i>p</i> (mm)
0.7	55	172	20	0.8
0.7	20	172	20	0.8
0.7	20	101	7	0.8
2.6	20	172	20	0.1
2.6	55	101	20	0.8
1.65	37.5	136.5	13.5	0.45
0.7	55	172	7	0.8
0.7	55	101	20	0.8
2.6	20	172	7	0.1
0.7	20	172	7	0.8
2.6	20	172	7	0.8
0.7	37.5	136.5	13.5	0.45
0.7	55	172	20	0.1
1.65	37.5	136.5	13.5	0.45
0.7	20	101	20	0.8
2.6	20	101	7	0.1
0.7	55	172	7	0.1
2.6	55	101	7	0.8
0.7	55	101	7	0.1
2.6	55	172	7	0.8
1.65	55	136.5	13.5	0.45
2.6	55	172	20	0.1
2.6	20	101	20	0.8
0.7	20	172	20	0.1
1.65	37.5	136.5	13.5	0.45
1.65	37.5	172	13.5	0.45
1.65	20	136.5	13.5	0.45
2.6	55	101	20	0.1
1.65	37.5	136.5	13.5	0.45
2.6	20	101	20	0.1
2.6	20	172	20	0.8
2.6	55	101	7	0.1
1.65	37.5	136.5	7	0.45
0.7	55	101	20	0.1
2.6	20	101	7	0.8
2.6	55	172	7	0.1
1.65	37.5	136.5	20	0.45
1.65	37.5	136.5	13.5	0.8
0.7	20	101	20	0.1
1.65	37.5	136.5	13.5	0.45
0.7	20	172	7	0.1
2.6	37.5	136.5	13.5	0.45
0.7	55	101	7	0.8
1.65	37.5	136.5	13.5	0.1
1.65	37.5	101	13.5	0.45
2.6	55	172	20	0.8
0.7	20	101	7	0.1

The force F_h is the resultant of two horizontal force components determined through vector sum as below:

$$F_h = \sqrt{F_a^2 + F_b^2} \tag{3}$$

where

F_a (N) is the force due to relative motion between the forming tool and sheet

F_b (N) is the thrust on the faces of pyramid

a and b are the two contiguous faces of pyramid.

Durante et al. [21] found that the force(s) in ISF continues to increase in the initial few contours due to dynamic equilibrium between sheet thinning and strain hardening. Therefore, they calculated the friction indicator once the force achieved steady state. The same approach was adopted in the present study. Moreover, while performing analysis, the force components in the central portion of wall were considered (as illustrated in Fig. 1c), and the spikes at the corners of pyramid were ignored.

The roughness tests were performed on the interior side of formed surfaces. The stylus travel was 6 mm, and the apparatus used for these tests was the M1 Maher Perthometer. The roughness was measured across the sheet stretching direction as indicated by an arrow in Fig. 1a. In view of their application in metal forming and computational modeling, four roughness quantities, namely R_a , R_z , R_{max} , and R_{eqv} were obtained. The former three were recorded on the Perthometer, while the last one was calculated using the below relation as detailed in [23]:

$$R_{eqv} = \frac{2}{d} \left(\frac{AR_z - BR_a}{\sin\theta/p} \right) \tag{4}$$

where

d (mm) is the tool diameter

θ (deg) is the forming angle

p (mm) is the step size

A (0.4) and B (0.6) are the two constants to weight R_a and R_z .

In order to identify the roughening mechanism in ISF, the surface morphology of unformed and formed surfaces was analyzed. This task was accomplished utilizing HITACHI SU3500 Scanning Electron Microscope (SEM).

3 Results and discussion

Because the dependence of roughness on various technological parameters is yet a subject of debate, significance of the considered parameters was identified for the current material. In this regards, analysis of variance (ANOVA) has been

practiced as a useful tool. As a step of ANOVA, power transformation on a response is applied in order to minimize the outlier's effects and thus to improve the efficacy of analysis [24]. However, this is done only when the lamada (λ) value in the related Box-Cox plot (a plot between lambda and Ln-residuals) does not meet the threshold value of 1. Therefore, to know the λ value, the Box-Cox plot for each of the presently considered five responses (i.e., μ' , R_a , R_z , R_{max} , R_{eqv}) was examined and accordingly an appropriate transformation was applied as listed in Table 3.

Table 4 presents the results of ANOVA. A term with prob value ≤ 0.05 (or 95% confidence level) was regarded as significant. This is to observe from the table that the flow stress Y_f , wall angle θ , and sheet thickness t , whose study was emphasized in the introduction, are significant for the roughness. These parameters, except the flow stress, are also influential for the friction indicator. The step size p with prob value < 0.0001 is the most significant parameter for both of the friction and roughness quantities. The rank of other parameters with respect to the significance can be judged based on the prob value: smaller the value, greater the significance will be. As observable from Table 4, some of the combinations of parameters are also significant, which signifies that the friction indicator and roughness in ISF is not simply determined by the sole effects of parameters instead interactive effects need to be taken into account in order to adequately understand their evolution.

3.1 Friction indicator

Figure 2a–d presents the effects of significant parameters on the friction indicator μ' . As can be noticed from Fig. 2a, b, the value of μ' increases as the thickness of sheet increases specifically when $\theta \leq 47^\circ$ and $d \leq 17$ mm. The value of μ' , however, slightly decreases with increasing thickness followed by a slight increase when $\theta > 47^\circ$ and $d > 17$ mm. This is to notice that the degree of importance of increasing thickness on the value of μ' comparatively decreases as the value of either of angle or diameter increases.

The effect of forming angle is observable from Fig. 2a, c. The value of μ' reduces with increasing the angle as long as the following conditions prevail: $d \leq 17$ mm and $t \leq 1.2$ mm. However, when $d > 17$ mm and $t > 1.2$ mm, the value of μ' slightly increases as the angle increases.

Figure 2b, d depicts the influence of tool diameter. Regardless of the interacting parameters (i.e., t and θ), the

value of μ' decreases as the diameter increases from 7 to 13.5 mm; however, μ' experiences an increase as the diameter increases from 13.5 to 20 mm. Figure 2d exhibits the influence of step size. The value of μ' steadily increases with an increase in the step size. The importance of increasing step size on μ' , however, decreases as the process is performed with the tools of greater diameters (say with $d > 7$ mm).

These findings reveal that the response of friction indicator to parameters variations is rather complex. In fact, the strain hardening of sheet and the tool/sheet contact area both experience a change when the forming is performed with an altered set of conditions [17]. These changes in turn affect the horizontal and vertical force components [17, 26] and hence the friction. Therefore, the reported behavior of friction indicator may be reasoned to the said variations.

3.2 Surface roughness

Figure 3a–l depicts the relationships between the technological parameters and the roughness quantities R_a , R_{max} , and R_z , respectively. As can be noticed from these figures, the set of parameters effects represented by Fig. 3a–d is similar to those depicted by Fig. 3e–l). This reveals that the effects of considered parameters on either of the mentioned roughness quantities are similar in nature. Therefore, only one of these roughness quantities namely, R_a is detailed herein study.

Figure 3a and b presents the response of R_a to variation in the thickness of sheet. The value of R_a consistently increases as the thickness increases. The increase in R_a , however, is relatively greater when ISF is performed at low angles (say $\theta \leq 37^\circ$) and with small diameters (say $d \leq 13.5$ mm).

The influence of forming angle on R_a is shown in Fig. 3a. The value of R_a decreases with increasing the forming angle especially when ISF is performed on high angle parts (say when $\theta \geq 28^\circ$). Figure 3b, c exhibits the effects of tool diameter on R_a . The value of R_a sharply decreases as the diameter increases from 7 to 13.5 mm. However, further increase in the diameter contrarily causes an increase in the value of R_a . The influence of increasing diameter, in terms of R_a , is greater when the thickness and step size are high (i.e., for $t \geq 1.65$ mm and $p \geq 0.45$ mm).

The effect of step size on R_a can be noticed from Fig. 3c. There is a consistent increase in the value of R_a as the step size increases. This increase, however, is greater when processing is done with low diameters (i.e., $d \leq 13.5$ mm). Figure 3d shows the role of flow stress of material on R_a . The value of R_a slightly reduces with an increase in the flow stress.

This is pertinent to mention that three parameters, which have been paid rare or limited attention in the literature as mentioned before, pose significant effects on the roughness of interior surface. Therefore, these parameters namely Y_f , θ , and t should be carefully considered to control the roughness in ISF.

Table 3 Transformations applied to various responses

Response	μ'	R_a	R_z	R_{max}	R_{eqv}
λ	0	1	0.39	0.33	0
Transformation	Ln	None	SQRT	SQRT	Ln

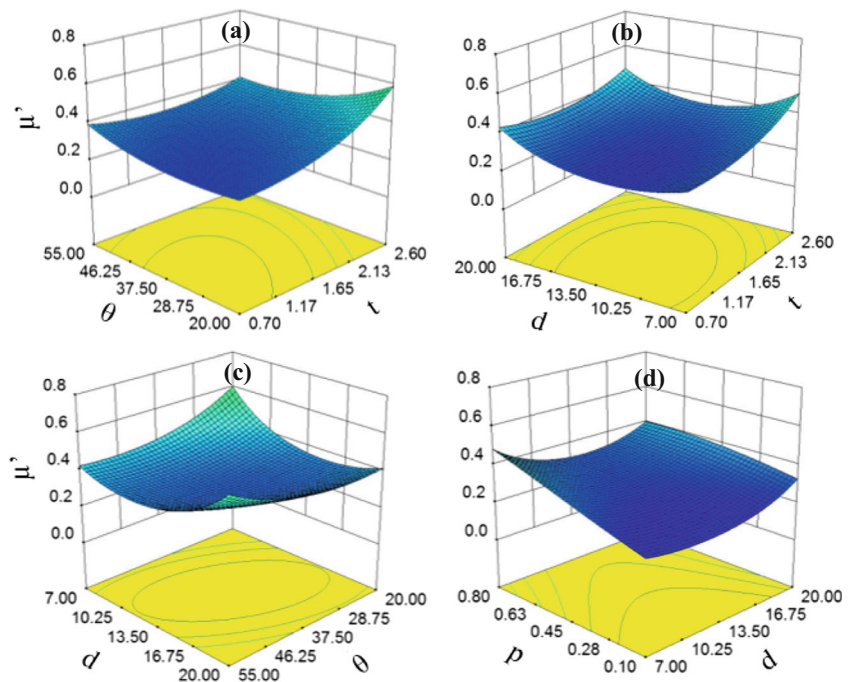
Table 4 Analysis of variance

Source	μ'		R_{max}		R_a		R_z		R_{eqv}	
	Prob value	S/NS	Prob value	S/NS	Prob value	S/NS	Prob value	S/NS	Prob value	S/NS
Model	<0.0001	S	<0.0001	S	<0.0001	S	<0.0001	S	<0.0001	S
t	0.002	S	<0.0001	S	<0.0001	S	<0.0001	S	<0.0001	S
θ	0.0082	S	0.0001	S	0.0005	S	0.0018	S	<0.0001	S
Y_f	0.4574	NS	0.05	S	0.0083	S	0.0376	S	0.0756	NS
d	0.1765	NS	<0.0001	S	<0.0001	S	<0.0001	S	<0.0001	S
p	<0.0001	S	<0.0001	S	<0.0001	S	<0.0001	S	<0.0001	S
$t\theta$	0.0004	S	0.0303	S	0.0407	S	0.0495	S	0.3343	NS
tY_f	0.436	NS	0.3626	NS	0.834	NS	0.2492	NS	0.1233	NS
td	0.0423	S	0.0013	S	0.0084	S	0.032	S	0.1096	NS
t_p	0.0533	NS	0.991	NS	0.1216	NS	0.9996	NS	0.0294	S
θY_f	0.9722	NS	0.5457	NS	0.2719	NS	0.5221	NS	0.7116	NS
θd	0.0001	S	0.1915	NS	0.3811	NS	0.9277	NS	0.6833	NS
θp	0.2899	NS	0.2558	NS	0.8976	NS	0.3577	NS	0.1144	NS
dY_f	0.6781	NS	0.3275	NS	0.2855	NS	0.137	NS	0.1103	NS
pY_f	0.4307	NS	0.4821	NS	0.425	NS	0.9488	NS	0.5936	NS
dp	0.001	S	0.0006	S	<0.0001	S	0.0026	S	0.079	NS
t^2	0.3016	NS	0.0485	S	0.2915	NS	0.2213	NS	0.2168	NS
θ^2	0.311	NS	0.0713	NS	0.0651	NS	0.108	NS	0.4421	NS
Y_f^2	0.7772	NS	0.834	NS	0.7852	NS	0.9989	NS	0.7748	NS
d^2	0.0333	NS	0.0032	S	0.0005	S	0.005	S	0.0051	S
p^2	0.6228	NS	0.1733	NS	0.0636	NS	0.0747	NS	<0.0001	S

S: significant

NS: not significant

Fig. 2 Relationships between friction indicator and parameters in ISF of Al1060 sheet: **a** forming angle and sheet thickness, **b** tool diameter and sheet thickness, **c** tool diameter and forming angle, and **d** step size and tool diameter



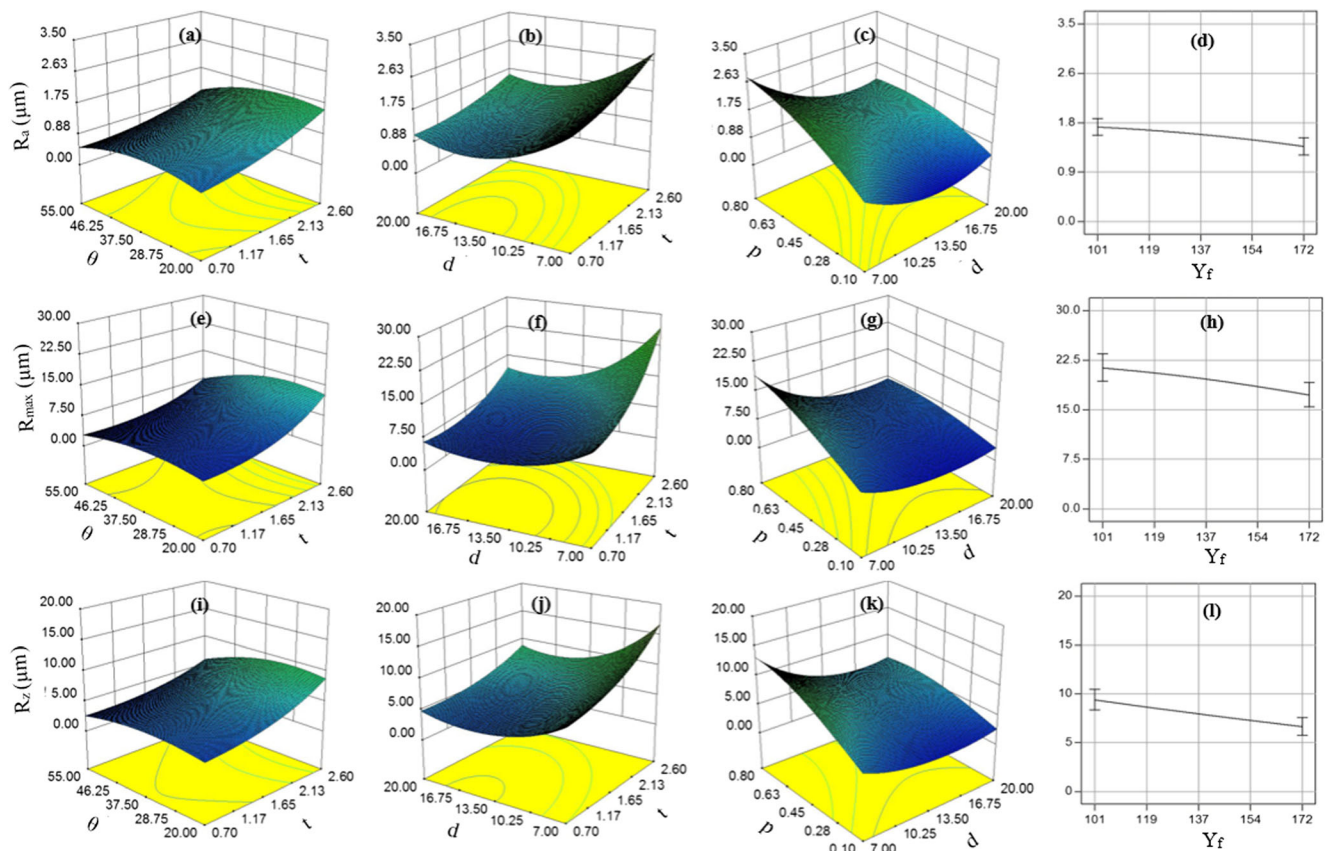


Fig. 3 Relationships between various roughness quantities and parameters in ISF of Al1060 sheet: **a–d** relation between mean roughness and parameters; **e–h** relation between maximum roughness parameters; and **i–l** relation between 10-point average roughness and parameters

Figure 4a–c depicts the effects of parameters on R_{eqv} , which is an empirical relation of R_a and R_z . This is to notice from Figs. 3 and 4 that R_{eqv} agrees with R_a , R_z , and R_{max} with respect to the response to variation in the step size and sheet thickness. However, its response to variation in the tool diameter and forming angle slightly differs in a sense that the nature of R_{eqv} contrary to those of R_a , R_z , and R_{max} is independent of the magnitude of these parameters (i.e., the value of R_{eqv} consistently decreases with an increase in either of these two parameters).

3.3 Analogy between the effects of parameters on friction and roughness, friction-roughness correlation, and morphology of formed surfaces

Table 1 (“current study” column) draws an analogy between the friction indicator μ' and roughness, especially R_a , with respect to their response to various parameters. As can be seen, most of the parameters have similar effects on the two. For an instance, an increase in the step size causes a

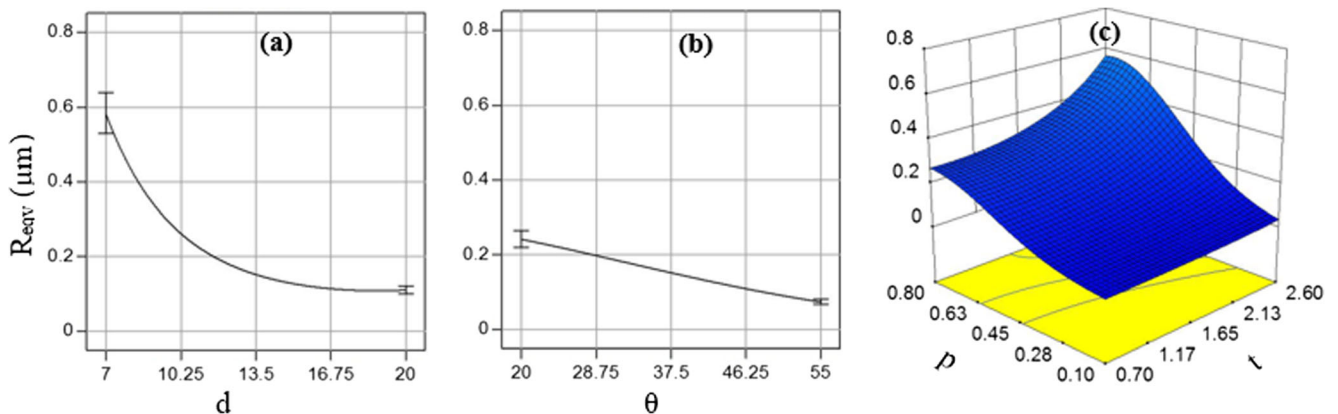


Fig. 4 Relationships between equivalent roughness and parameters in ISF of Al1060 sheet: **a** tool diameter, **b** forming angle, and **c** step size and sheet thickness

corresponding increase in the roughness. The same trend is observed for the friction. Similarly, analogous responses can be seen as the tool diameter is varied. Regarding response to thickness, analogy in the friction and roughness is realized as long as $\theta \leq 47^\circ$ and $d \leq 17$ mm. The analogy in respect of response to the forming angle is also linked with certain conditions, i.e., $d \leq 17$ mm and $t \geq 1.2$ mm. These conditions, however, are very close to the high limits of parameters employed herein work (e.g., high limit of θ is 55° and that of d is 20 mm) and thus allow to claim that the friction and roughness principally exhibit analogous responses to the technological variations.

Figure 5 plots the mean roughness as a function of friction indicator. The roughness in general linearly increases as the friction indicator increases. In fact, as can be observed from the SEM-based morphology of representative formed surfaces presented in Fig. 6a–f, the sheet abrasion (or wear) due to sliding action of the forming tool increases as the friction increases. This consequently results into increased roughness. Based on this finding and the analogy drawn above in the responses of friction and roughness, it is possible to say that the friction has controlling influence on the roughening of interior surface of the experimental sheet. The said influence of friction in ISF is consistent with that in the stretch-bending operation whereby an increase in the friction has been observed to correspondingly roughen the surfaces [27]. This consistency in the two processes might be attributed to their alike mechanics, i.e., sheet in both of the processes is subjected to stretching and bending. This is pertinent to point out that the reader may not confuse the friction indicator μ' , used in the present study, with the friction coefficient μ . The value of μ' could be greater than 1, as found in the present study and reported in the ISF literature [21, 22], whereas the value of μ is usually smaller than 1. In fact, this indicator is only an estimation of friction rather than an exact value of friction at the tool/sheet interface.

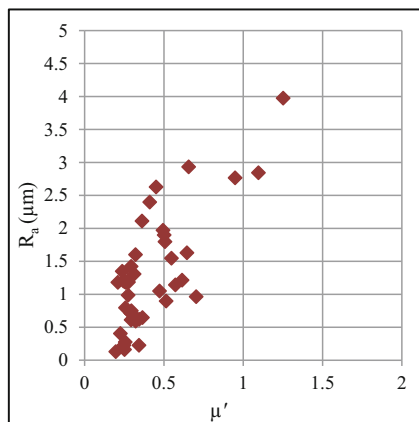


Fig. 5 Relationship between mean roughness and friction indicator determined for Al1060 sheet

From Table 4, this is to notice that the flow stress appears to be a significant parameter for the roughness while an insignificant one for the friction indicator. Undoubtedly, the forming force increases as the flow stress increases. However, this increase is realized in both of the horizontal (F_h) and vertical (F_v) components of force. As a result, the ratio of these two force components (regarded as friction indicator) does not experience any substantial change. This point is also supported by Fig. 3d, whereby it can be observed that the flow stress has only a subtle effect on the roughness.

3.4 Parameter-combination having controlling influence on the roughness

Figure 7 presents the mean roughness as the function of various empirical combinations of parameters. The appropriateness of a function is dictated by the R^2 value: a higher value shows better fit to the data points. The relation between R_a and $d/2p$ has an R^2 value of 63%. The addition of θ (i.e., $d\sin\theta/2p$), however, improves the R^2 value from 63 to 67%. The addition of $1/t$ to $d/2p$ (i.e., $d/2pt$) enhances the R^2 value from 63 to 77%. The unification of the latter two combinations (i.e., $d\sin\theta/2pt$) yields the highest R^2 value of 82%. From the R^2 values, it follows that the factor $d/2p$ has the greatest contribution on the roughening of interior surfaces, which is followed by the factors $1/t$ and $\sin\theta$. Interestingly, all of the mentioned combinations are related to the roughness through the power law.

In order to examine if the other roughness quantities, namely R_{max} , R_z , and R_{eqv} are sensitive to the combination $d\sin\theta/2pt$, their correlations with the said combination were examined. As shown in Fig. 8, each of the considered quantities forms a reasonable relation with $d\sin\theta/2pt$. However, that of R_{eqv} having the highest R^2 value (i.e., 90%) is the most consistent one. The behavior of R_a and R_{eqv} as the function of $d\sin\theta/2pt$ can be defined by the following formulas:

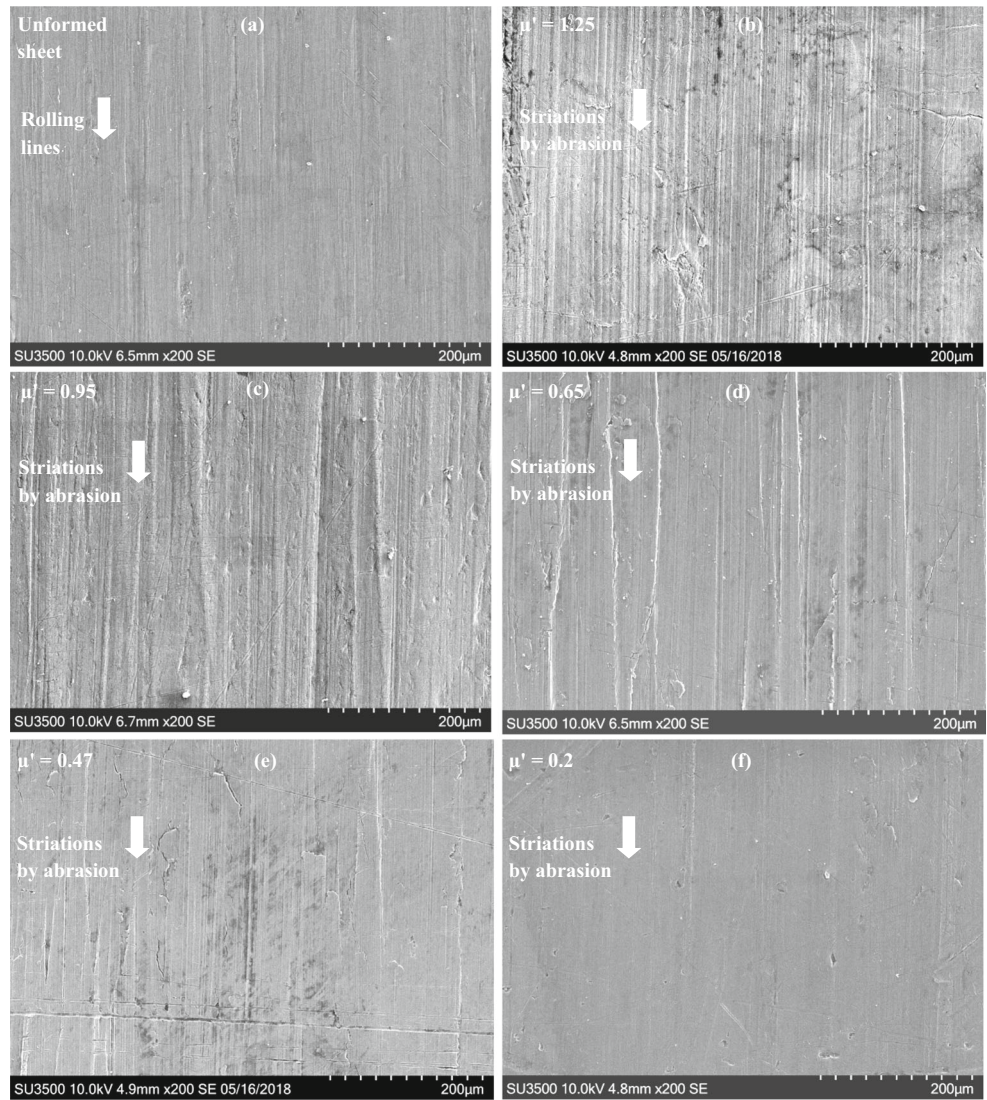
$$R_a = 3.21(d\sin\theta/2pt)^{-0.65} \tag{5}$$

$$R_{eqv} = 1.75(d\sin\theta/2pt)^{-1.29} \tag{6}$$

The R^2 value for R_a and R_{eqv} is 82 and 90%, respectively. These values are reasonably high and indicate a good fit of respective data to be reliably used for the prediction and optimization of the surface roughness of Al1060 sheet.

The application of the above proposed combination to other materials was examined by employing a composite sheet having higher flow stress (i.e., $Y_f = 115$ to 177 MPa). In fact, to evaluate the residual stresses in another study, the authors had produced a series of pyramids from the Cu/steel composite sheet. The roughness was measured from these pyramids across the stretching

Fig. 6 Surface morphology of selected surfaces with various values of friction indicator: **a** unformed sheet, **b** $\mu' = 1.25$, **c** $\mu' = 0.95$, **d** $\mu' = 0.65$, **e** $\mu' = 0.47$, **f** $\mu' = 0.2$



direction. For the process conditions and other details, the reader is referred to Fig. 9 and the related article [28]. As presented in Fig. 9, the roughness of interior surface of

Cu/steel sheet is also sensitive to $d\sin\theta/2pt$. This follows that the proposed parameter-combination is an appropriate factor having controlling effect on the interior roughness

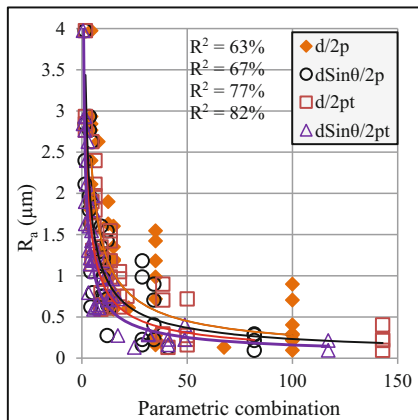


Fig. 7 Relationships between mean roughness and various empirical combinations determined for Al1060 sheet

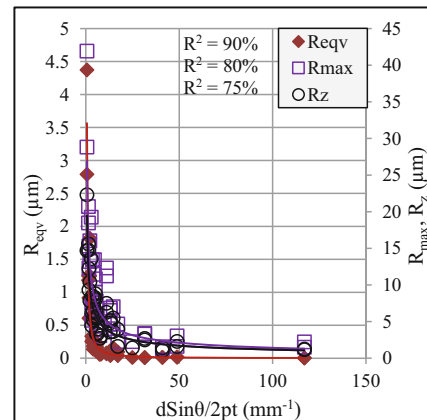


Fig. 8 Relationships between $d\sin\theta/2pt$ and various roughness quantities determined for Al1060 sheet

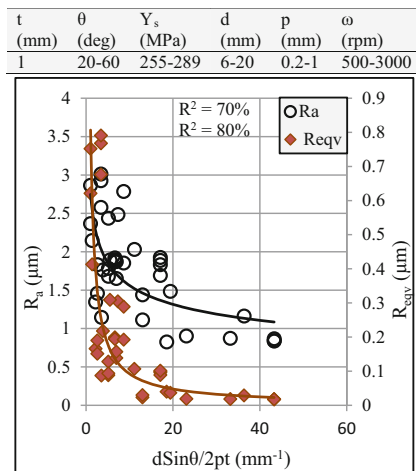


Fig. 9 Relationship between $d\sin\theta/2pt$ and surface roughness determined for Cu/steel composite sheet

in ISF. The formulas of R_a and R_{eqv} for the Cu/steel sheet are as given below:

$$R_a = 2.76 (d\sin\theta/2pt)^{-0.248} \tag{7}$$

$$R_{eqv} = 0.827(d\sin\theta/2pt)^{-0.953} \tag{8}$$

The R^2 value of these two formulas is 70 and 80%, respectively. These values are low in comparison to those obtained for Al1060 sheet. This discrepancy is due to a reason that the roughness data of Cu/steel sheet include two additional effects due to rotation (ω) and feed rate (f) besides that of $d\sin\theta/2pt$. This dictates the need of incorporating these effects into $d\sin\theta/2pt$ to formulate a combination valid under generic conditions. This task is left for future, however. From Figs. 7–9, it is worth noticing that the value of $d\sin\theta/2pt$ should be kept smaller for minimizing the roughness. Moreover, the threshold value (the value below which the roughness remains almost constant) is dependent upon the material, i.e., around 50 mm^{-1} for the Al10160 sheet (low flow stress) and about 20 for the Cu/steel composite sheet (high flow stress). This means that a high-strength material may have lesser threshold value; however, this point needs to be ascertained employing additional materials.

The above idea to formulate an empirical combination of parameters to control the roughness of interior surface stems into the work by Hamilton and Jeswiet [23], whereby they successfully correlated the roughness of exterior surface with a parameter-combination $d\sin\theta/2p$. As an objective of the current study, the suitability of $d\sin\theta/2p$ for the interior surface was tested considering Al1060 sheet. As shown in Fig. 7, the R^2 value for the plot between $d\sin\theta/2p$ and R_a is only 67% (i.e., a lack of fit of 33%). The incorporation of the factor $1/t$ into this combination, i.e., $d\sin\theta/2pt$, enhances the data fit from 67 to 82% (i.e., 15% improvement). Thus, this study introduces a new factor $1/t$ and also reveals such a combination for the interior surface in addition to the exterior surface reported in [23].

3.5 Comparison between the present and past roughness studies

Table 1 summarizes the present and past roughness findings in ISF. The review of the previous findings was presented in Sect. 1. Therefore, this section only compares the present and past findings. The present study reports that the mean roughness R_a of Al1060 sheet increases as the step size increases from 0.1 to 0.8 mm. This trend completely agrees with that observed in Al1050 [16], Al3003 [15], and Al70750 [17]. The same partially agrees with Al5052 [18, 20] (i.e., disagrees for certain range of step size). However, the present finding regarding the step size completely disagrees with that reported for AISI304L despite the fact the sheet of AISI304L was formed with an equivalent step size (say 0.8 mm) and relatively smaller diameter (say 8 mm) as opposed to 20 mm in the present study. The influence of tool diameter found for the current Al1060 sheet is consistent with that reported for Al70750 [21], partially consistent with the result for Al1050, but completely inconsistent with the finding reported for AISI304L [19]. This analysis allows inferring that the nature of influence of a parameter is closely associated to the type of material under study. In fact, the interaction and the friction between the contacting surfaces depend upon the type of material. As a result, the friction coefficient changes with the type of material thus leading to change in the roughening behavior of sheet during forming.

Figure 10 depicts the correlations of R_a with the other roughness quantities. As can be noticed, the roughness R_a holds a direct relation with either of R_z or R_{max} . This explains why the nature of effects of technological parameters, presented in Fig. 3, is similar for these three roughness quantities. The relation between R_a and R_{eqv} is defined by the exponential law. The value of either of R_z , R_{max} , or R_{eqv} increases as the value of R_a increases.

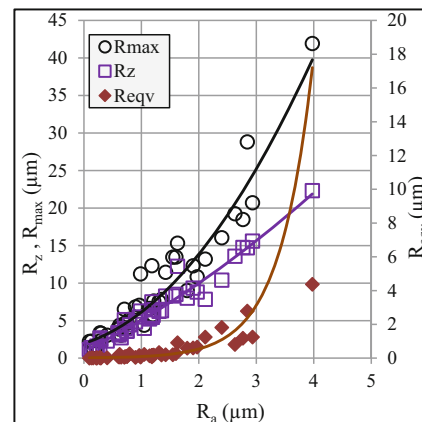


Fig. 10 Relationship among various quantities of roughness in ISF of Al1060 sheet

4 Conclusions

The nature of influence of ISF processing on surface roughening has not yet been agreed upon. More efforts need to be spent to comprehend the threshold knowledge. In the present study, the friction at the tool/sheet interface and the roughening behavior of interior surfaces were investigated. The following conclusions can be drawn from the study:

1. A parameters-combination, i.e., $d\sin\theta/2pt$, having controlling influence on the roughening of interior surfaces has been proposed and validated employing two materials. The roughness decreases as a power function of the said combination. An optimum value of 50 mm^{-1} is proposed to be maintained in order to produce the quality components of Al1060 sheet and a value of 20 mm^{-1} for the laminated Cu/steel composite.
2. The analogy between the roughness and friction indicator, in respect of their response to parameters, dictates that the roughening of interior surface mainly occurs due to friction at the tool/sheet interface. Further, according to the correlation, the roughness linearly increases with increasing the friction indicator because the surface abrasion correspondingly increases as revealed by the SEM-based morphology of the formed surfaces.
3. Some of the sparsely investigated parameters, namely flow stress of material, sheet thickness, and forming angle, have shown significant impact on the roughness of interior surface. These effects are interactive in nature and need to be carefully undertaken so as to realize the good surface finish.
4. There is a discrepancy between the current and previous roughness findings reported in the ISF literature. In this regards, the type of material has appeared as the major factor that affects the tool/sheet interaction (or friction condition) and hence the roughness.

Funding information This research work was supported by the Fundamental Research Funds for the Central Universities (Grant No.: NS2015054) PR China and State Administration of Foreign Experts Affairs PR China and Ministry of Education PR China (111 project, Grant No.: B16024).

Publisher's Note Springer Nature remains neutral with regard to jurisdictional claims in published maps and institutional affiliations.

References

1. Powell N, Andrew C (1992) Incremental forming of flanged sheet metal components without dedicated dies. *Proc IMechE B J Eng Manuf* 206:41–47
2. Jeswiet J, Hagan E (2001) Rapid proto-typing of a headlight with sheet metal. *Proceedings of Shemet Conference* 165–170
3. Ambrogio G, Filice L, Gagliardi F (2012) Improving industrial suitability of incremental sheet forming process. *Int J Adv Manuf Technol* 58:941–947
4. Li J, Bai T, Zhou Z (2014) Numerical simulation and experimental investigation of incremental sheet forming with an elastic support. *Int J Adv Manuf Technol* 74:1649–1654
5. Fan G, Gao L, Hussain G, Wu Z (2008) Electric hot incremental forming: a novel technique. *Int J Mach Tools Manuf* 48:1688–1692
6. Dufflou JR, Callebaut B, Verbert J, Baerdemaeker HD (2008) Improved SPIF performance through dynamic local heating. *Int J Mach Tools Manuf* 48:543–549
7. Echriif SBM, Hrairi M (2011) Research and progress in incremental sheet forming processes. *Mater Manuf Process* 26:1404–1414
8. Jeswiet J, Micari F, Hirt G, Bramley A, Dufflou J, Allwood J (2005) Asymmetric single point incremental forming of sheet metal. *Ann CIRP* 54:623–650
9. Gatea S, Ou H, McCartney G (2016) Review on the influence of process parameters in incremental sheet forming. *Int J Adv Manuf Technol* 87:479–499
10. Kim YH, Park JJ (2002) Effect of process parameters on formability in incremental forming of sheet metal. *J Mater Process Technol* 130/131:42–46
11. Hussain G, Gao L, Hayat N, Cui Z, Pang Y, Dar NU (2008) Tool and lubrication for negative incremental forming of a commercially pure titanium sheet. *J Mater Process Technol* 203:193–201
12. Lu B, Fang Y, Xua DK, Chen J, Oub H, Moser MH, Cao J (2014) Mechanism investigation of friction-related effects in single point incremental forming using a developed oblique roller-ball tool. *Int J Mach Tools Manuf* 85:14–29
13. Hussain G, Gao L, Zhang ZY (2008) Formability evaluation of the pure titanium sheet in the cold incremental forming process. *Int J Adv Manuf Technol* 37:920–926
14. Lu B, Chen J, Ou H, Cao J (2013) Feature-based tool path generation approach for incremental sheet forming process. *J Mater Process Technol* 213:1221–1233
15. Hagan E, Jeswiet J (2004) Analysis of surface roughness for parts formed by computer numerical controlled incremental forming. *Proc IMechE J Eng Manuf* 218:1307–1312
16. Echriif SBM, Hrairi M (2014) Significant parameters for the surface roughness in incremental forming process. *Mater Manuf Process* 29:697–703
17. Durante M, Formisano A, Langella A (2011) Observations on the influence of tool-sheet contact conditions on an incremental forming process. *J Mater Eng Perform* 20:941–946
18. Mugendiran V, Babu AG, Ramadoss R (2000) Parameter optimization for surface roughness and wall thickness on AA5052 aluminium alloy by incremental forming using response surface methodology. *Process Eng* 97:1991–2000
19. Cavalier LCC, Schaeffer L, Rocha AS, Peruch F (2010) Surface roughness in the incremental forming of AISI 304L stainless steel sheets. *Far East J Mech Eng Ph* 1:87–98
20. Baruah A, Pandivelan C, Jeevanantham AK (2017) Optimization of AA5052 in incremental sheet forming using grey relational analysis. *Measurement* 106:95–100
21. Durante M, Formisano A, Langella A, Memola F, Minutolo C (2009) The influence of tool rotation on an incremental forming process. *J Mater Process Technol* 209:4621–4626
22. Xu D, Wu W, Malhotra R, Chen J, Lu B, Cao J (2013) Mechanism investigation for the influence of tool rotation and laser surface texturing (LST) on formability in single point incremental forming. *Int J Mach Tools Manuf* 73:37–46
23. Hamilton K, Jeswiet J (2010) Single point incremental forming at high feed rates and rotational speeds: surface and structural consequences. *CIRP Ann—Manuf Technol* 59:311–314
24. Montgomery DC (1997) *Design and analysis of experiments*, 4th edn. Wiley, New York

25. ASTM Book of Standards Volume 03.01 (2018) Metals—mechanical testing; elevated and low-temperature tests; Metallography
26. Al-Ghamdi KA, Hussain G (2015) Forming forces in incremental forming of a geometry with corner feature: investigation into the effect of forming parameters using response surface approach. *Int J Adv Manuf Technol* 76:2185–2197
27. Shi X, Hussain G, Butt Shahid I, Song F, Huang D, Liu Y (2017) The state of residual stresses in the Cu/steel bonded laminates after ISF deformation: an experimental analysis. *J Manuf Process* 30:14–26
28. Azushima A, Sakuramoto M (2006) Effects of plastic strain on surface roughness and coefficient of friction in tension-bending test. *Ann CIRP* 55:303–306